Beyond the empirical pillar design method: The strain criterion and the pillar load inversion concepts

by K.B. Le Bron[1], L.J. Gardner[2], and J. van Zyl[3]

Affiliation:
[1]MLB Consulting, Ballito, South Africa
[2]Impala Platinum Ltd, Rustenburg, South Africa
[3]Glencore Alloys, Rustenburg, South Africa

Correspondence to:
K.B. Le Bron

Email:
kevin@mlbconsulting.co.za

Dates:
Received: 5 Sept. 2023
Revised: 24 Nov. 2023
Accepted: 13 Feb. 2024
Published: May 2024

How to cite:
Le Bron, K.B., Gardner, L.J., and van Zyl, J. 2024. Beyond the empirical pillar design method: The strain criterion and the pillar load inversion concepts. *Journal of the Southern African Institute of Mining and Metallurgy*, vol. 124, no. 5. pp. 293–302

DOI ID:
http://dx.doi.org/10.17159/2411-9717/3125/2024

Abstract

Pillar design is a crucial aspect of underground mining engineering, as it directly impacts the safety, stability, and overall effectiveness of mining operations. In this paper we present a method to calculate pillar stability based on the strain criterion and pillar load inversion concept, which complements the empirical pillar strength formulae. Those formulae do not account for certain parameters that can affect the stability of the pillars, e.g. weak layers, changes in stress orientations due to mining, orebody dip, mining layout complexity, and the influence of regional stabilizing pillars. The approach presented here is not intended to replace the empirical method; rather, we suggest using it as the initial step in the pillar design process. This should be followed by iterative numerical modelling to study pillar behaviour, define pillar stability, and optimize the pillar design by considering site-specific and representative rock mass properties and criteria.

Keywords

pillar design, strain criterion, tabular orebody, bord and pillar

Introduction

Pillars are unmined portions of ore that are left in place to support the roof and overburden. These pillars help to minimize the risk of roof collapses, which could injure people working in underground excavations. Correctly designed pillars provide support to prevent subsidence (applicable to shallow mining conditions) and maintain the integrity of the surrounding rock mass.

The stability of the walls of an excavation relies on the pillar layout. The size and location of pillars can impact the efficiency of resource extraction. If pillars are too large, significant amounts of valuable resources will be left unmined. On the other hand, if they are too small, they could fail and compromise stability.

The extraction method used in underground mining, e.g. the bord-and-pillar approach, determines the layout and design of the pillars. Each mining method involves specific pillar design considerations. Pillar design is therefore a crucial aspect of underground mining engineering. In this paper we present a pillar design method that goes beyond the empirical approach by incorporating a strain criterion concept and a pillar load inversion concept.

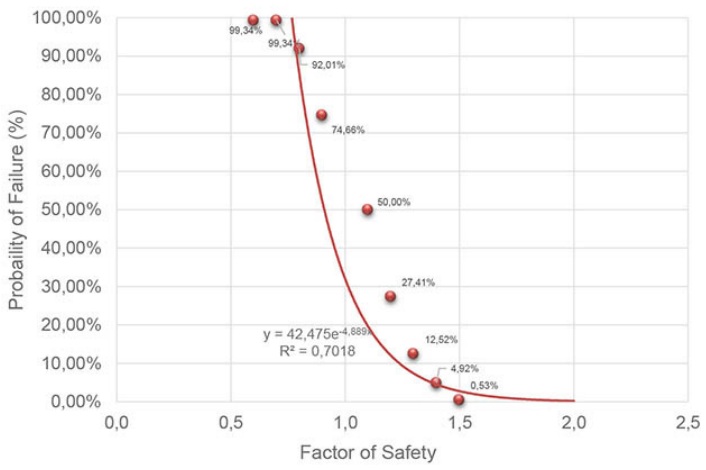

Figure 1—The relationship between predicted probability of failure and the factor of safety of coal pillars (after Salamon and Munro, 1967)

Beyond the empirical pillar design method: The strain criterion and the pillar load inversion concepts

Salamon and Munro (1967) followed an empirical approach, which involved studying data from a total of 125 pillars in South African coalfields, 27 of these being collapsed pillars. Based on a statistical appraisal of the data, they presented a relationship between the probability of failure (PoF) and factor of safety (FoS) for coal pillars. The graph presented in Figure 1 is based on this data, which also forms the basis for applying a factor of safety of 1.6 in coal pillar design.

Several empirically based pillar strength equations have since been developed for hard rock mines (Hedley and Grant, 1972; von Kimmelman, Hyde, and Madgwick, 1984; Lunder and Pakalnis, 1997). Hedley and Grant (1972) specifically applied the approach adopted by Salamon and Munro (1967) to develop a pillar strength formula hard rock mines, based on a study of 28 pillars (three of which were defined as failed) at the Elliot Lake uranium mines in Canada. This formula has typically been used for designing pillars for mines in the Bushveld Complex.

The empirical strength formulae have several limitations.

- They are mostly based on the study of a limited number of pillars, and the interpretation of 'stable' versus 'failed' pillars is not always clear,
- They are designed for a particular orebody, and are not necessarily applicable in other, potentially similar orebodies,
- They do not account for parameters that may impact the stability of the pillars, such as weak layers, changes in stress orientations as a result of mining, orebody dip, complexity of mining layout, and the effect of regional stabilizing pillars.

Kersten (2019) suggested that the application of the empirical Hedley-Grant formula in conjunction with tributary area theory requires revision. He investigated the possibility of creating an analytical solution to replace the empirical approach, using the load line of the pillar system in conjunction with FLAC2D modelling and the Hoek-Brown (1980) failure criterion, to calculate pillar deformation and failure strength. He concluded that this method may be used to predict the influence of rock mass characteristics, the likelihood of pillar failures at greater depths, and alternative pillar mining methods.

Malan (2010) concluded that neither empirical techniques nor numerical modelling currently provide a solid basis for conducting pillar design. He therefore recommended that both these techniques be utilized to obtain the best possible insight into the problem. Napier and Malan (2011) cite uncertainties in pillar strength and loading stiffness as reasons for moving beyond the sole use of empirical formulae for pillar design towards combining monitoring and numerical modelling to obtain the best insights into design problems (Spottiswoode and Drummond, 2014).

The approach suggested in this paper is a hybrid methodology for pillar design. It is not intended to replace the empirical method; rather, it incorporates both empirical methods and inelastic numerical modelling, applying the strain criterion concept and pillar load inversion concept. We thus recognize the value of empirical data, but propose that it should be utilized as the initial phase of pillar design.

Subsequently, numerical modelling is introduced to further assess and understand pillar behaviour, allowing for a more accurate definition of pillar stability. This is achieved by considering rock mass properties and stability criteria that are specific to the site in question and which accurately represent the rock mass and loading conditions. The components required in the pillar design process are presented in Figure 2.

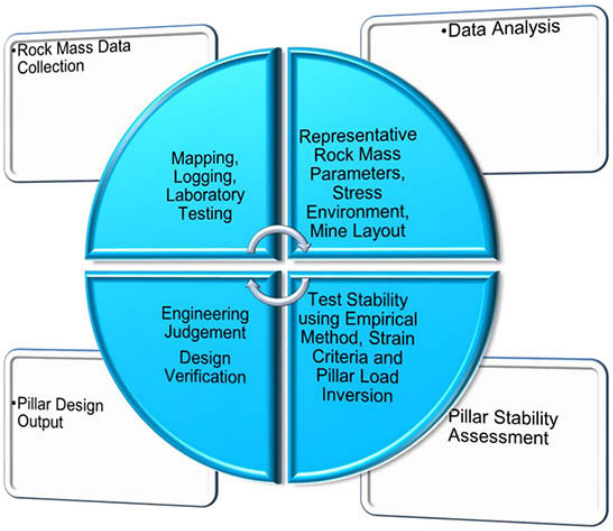

Figure 2—Components of the hybrid pillar design process

Confidence in the design improves with increasing understanding of the rock mass data. With access to accurate and comprehensive data relating to the rock mass, including geological characteristics, structural features, mechanical properties, and potential hazards, more informed decisions are possible during the design phase.

The available advanced geotechnical modelling techniques allow geotechnical engineers to simulate different scenarios, assess rock mass behaviour under a range of conditions, and identify potential challenges before any excavation is developed. Thus, with accurate rock mass data, the numerical models and empirical methods become more reliable and can provide insights into potential challenges that might arise during the mining operation.

As the empirical method is well-known and widely used, the novel pillar load inversion concept and strain criterion are presented together with case studies that best illustrate their application.

The concept of pillar load inversion

Under elastic conditions, the stresses along the edges and at the corners of pillars are considerably higher than at the core of the pillar. During mining, pillars may become overloaded, which may lead to load shedding at the pillar (or excavation) edges and particularly the pillar corners.

When load shedding occurs at the corners, the pillar load is transferred to the confined core. As the load on the pillar is further increased, the stress profile changes from being higher near the pillar edge to a peak at the pillar centre (Figure 3). This implies that load inversion has occurred in the pillar, meaning that the pillar behaviour has transitioned from elastic to inelastic.

If the pillar edges remain within the elastic zone, this situation will indicate stable pillar conditions. However, fracturing on the pillar edge does not necessarily mean pillar failure. Since there may be two intersections on the pillar stress curve for the same stress level (Figure 4), i.e. one in the elastic zone and the other post-failure, the strain would be the determining factor for failure. A graphical explanation of the concept is indicated in Figures 3 and 4.

Axial strain criterion based on uniaxial compressive strength (UCS) tests

The positive axial strain at failure can be used to predict potential failure in the rock mass where similar unconfined conditions may

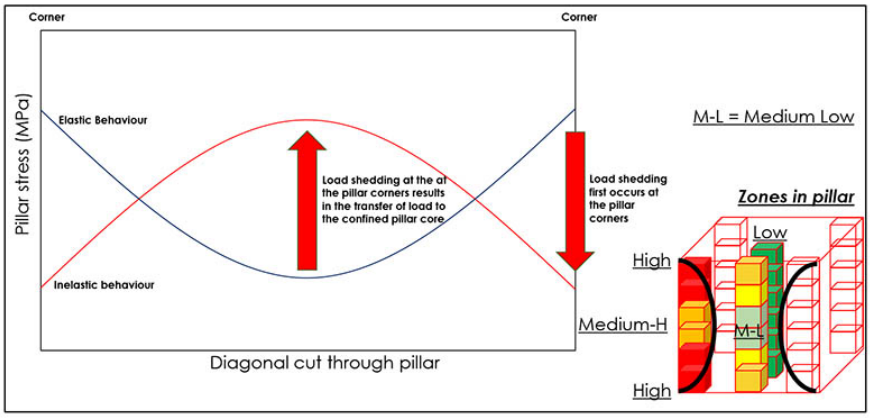

Figure 3—Illustration of the concept of pillar load inversion via a section through a pillar. Brittle failure occurs at the pillar corners, extendung to the pillar core

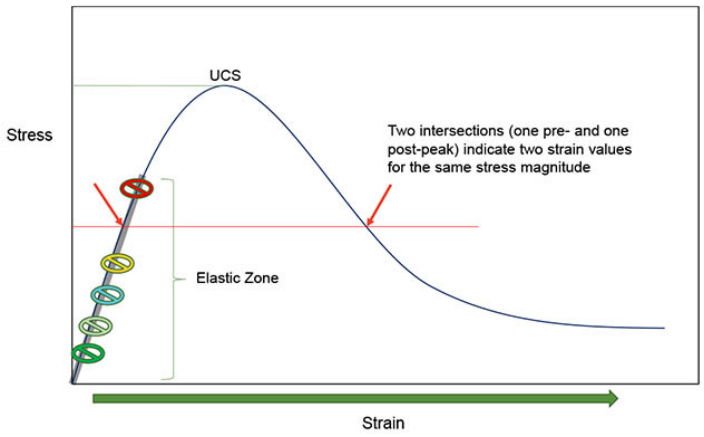

Figure 4—Stress-strain curve, showing the concept of pillar load inversion based on compression

exist. The strain criterion has been applied successfully to predict potential pillar instabilities on mines located in the Bushveld Complex (described in numerous project reports submitted to various mines and which are not publicly available).

The edges of underground pillars may experience similar unconfined compression to samples tested in the laboratory. This means that the vertical axial strain may be applied as a stability condition in inelastic numerical modelling to determine the onset of pillar fracturing as a precursor to possible slabbing and spalling of the pillar sides (this is based on underground measurements from five pillar formation and pillar reduction projects).

A conservative approach to pillar design would assume a minimum value for axial strain, determined during UCS tests in a laboratory (it should be noted that higher width-to-height ratios may lead to pillar punching or strain bursting in some rock types, which is not discussed in this paper). Using the median or average UCS strain may be more appropriate, as it is more representative of an entire system of pillars. For the adoption of this approach, a large database of laboratory test data is preferable, as it improves confidence in the data and allows representative rock mass parameters and failure criteria to be compiled.

One of the Bushveld Complex mines has a substantial laboratory testing database which was used to illustrate the criteria. The graphs in Figures 5 and 6 show a probabilistic approach to the available laboratory-determined UCS strain data for Merensky Reef samples. These graphs are based on available laboratory-tested axial strain data for Merensky pyroxenite (MPX - Figure 5) and Merensky pegmatoid (MPG - Figure 6) samples. The minimum values are predicted to be approximately 1.2 mm/m for both MPG and MPX. Provided the minimum value for strain at failure is not exceeded, the pillar is predicted to remain in the elastic zone. The average values are approximately 2.2 mm/m for MPX and 1.75 mm/m for MPG.

Axial strain criterion based on triaxial confinement

The relationship between confining stress and triaxial compressive strength is presented in Figures 7 and 8, for MPX and MPG, respectively. The graphs indicate that an increase in confinement will result in significantly greater rock strengths. For MPX, the average UCS (without confinement) is approximately 117 MPa, increasing to approximately 275 MPa for a pillar confinement of 20 MPa. For MPG, the average UCS is approximately 96 MPa, increasing to approximately 195 MPa for a pillar confinement of 20 MPa. It is noted that at a pillar confinement of 40 MPa, the compressive strength is predicted to be as high as 275 MPa.

The effects of confinement on the vertical axial strain are presented in Figures 9 and 10. The graphs show that confining stresses of 20 MPa or higher will result in a vertical axial strain at failure of approximately 6 mm/m. Increased confinement not only results in greater axial compressive strength, but also increased strain deformation before sample failure.

Figure 9, therefore, suggests that for a horizontal confining stress of at least 20 MPa, a strain criterion of approximately 6 mm/m (or millistrain) may be applied anywhere in the pillar where the

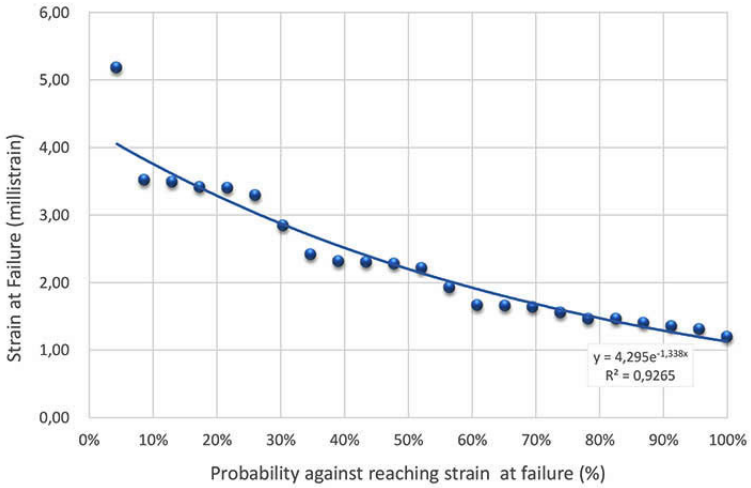

Figure 5—Probability analysis of failure strain (based on laboratory UCS testing) for Merensky pyroxenite (MPX)

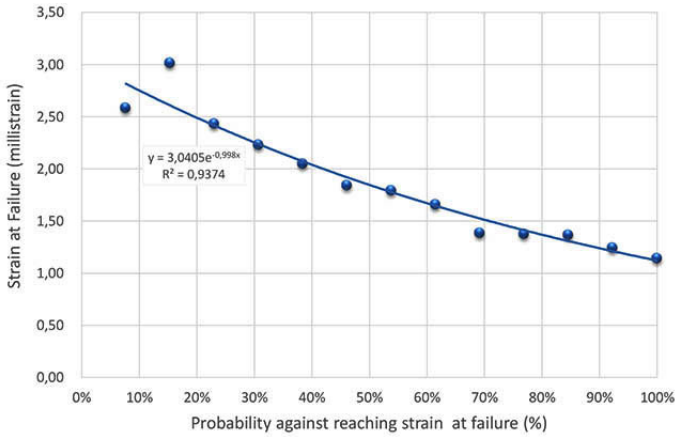

Figure 6—Probability analysis of failure strain (based on laboratory UCS testing) for Merensky pegmatoid (MPG)

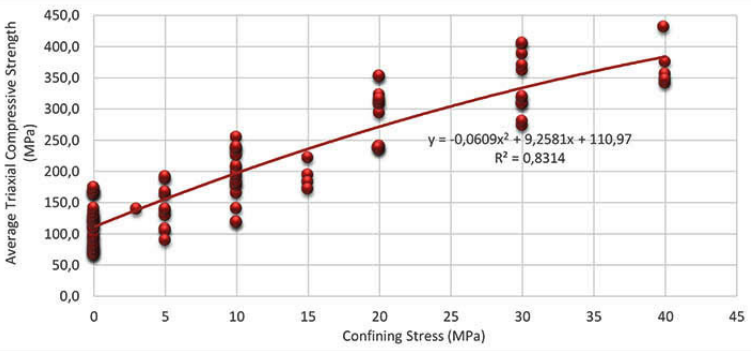

Figure 7—Effect of confining stress on the triaxial compressive strength of Merensky pyroxenite (MPX)

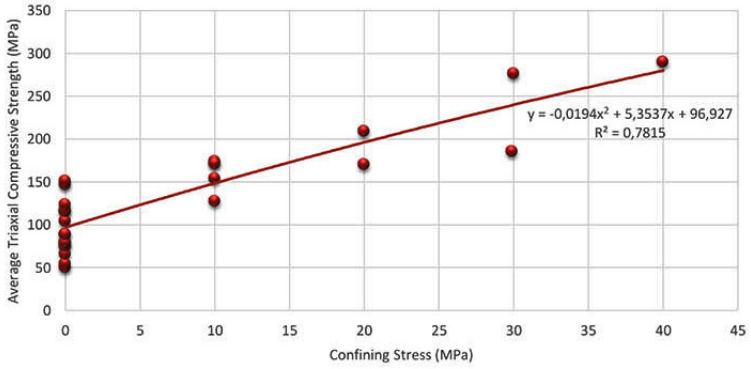

Figure 8—Effect of confining stress on the triaxial compressive strength of Merensky pegmatoid (MPG)

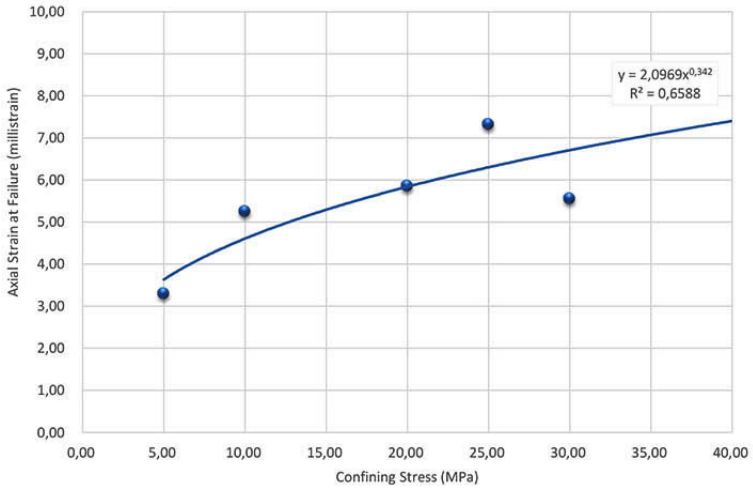

Figure 9—Effect of confining stress on axial strain at failure

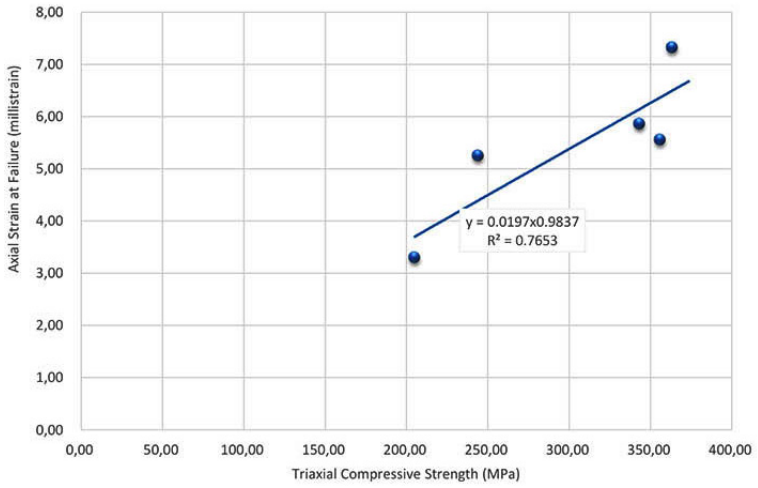

Figure 10—Relationship between axial strain at failure and triaxial compressive strength

confinement is equivalent to that value, as an indication of the potential onset of fracturing. which may result in load shedding of that particular zone (under triaxial loading). At confining stress levels of approximately 95 MPa, the criterion would be 10 millistrain.

Case study 1: Application in a bord-and-pillar layout on the Merensky Reef at depths of 1270–1350 m below surface

FLAC3D Itasca Consulting Croup, 2014) was used to evaluate the pillar stability for the bord-and-pillar layout with regional stabilizing pillars on the Merensky Reef at depths down to 1350 m below surface. The dimensions of the regional stabilizing pillars, namely 14 m × 14 m, were determined using the empirical strength formula. These pillars are non-continuous, due to ventilation requirements and restrictions posed by mechanical equipment and mine layout. In-stope pillars were simulated as 7 m × 7 m, 7.5 m × 7.5 m, and 8 m × 8 m, in each case with 7 m bords and a mining height of 1.85 m. A total of 11 bords were included between the regional stabilizing pillars. The Mohr-Coulomb constitutive model was assigned to all rock mass types simulated (over Hoek-Brown), with the material properties being derived from laboratory tests, core logging, and underground mapping data and observations. Detailed site-specific data was available to realistically represent the rock mass in the model, as shown in Figure 11. Saiang et al. (2014) state that Hoek-Brown model is not a classic constitutive model like the Mohr-Coulomb and hence, cannot relate stress and strain the same way as the Mohr-Coulomb model. Saiang et al. (2014 further state that Hoek-Brown will have the tendency to produce questionable results when large plastic strains occur. For strain softening to be attempted applying this approach, one would need post-peak residual strength properties. The associated friction angle and cohesion at the residual strength, would have to be determined by running sensitivity analyses until representative residual strength parameters are obtained. This information is not available, which is why Mohr Coulomb Constitutive model was run. The pillar load inversion concept and strain criterion were applied to determine pillar stability in the models. The following data was used to define the onset of fracturing and pillar failure:

- Unconfined pillar sides/corners – vertical strain of 1.75 mm/m (MPG average)
- Confined pillar core – vertical strain of 6 mm/m
- Triaxial compressive stress – 195 MPa (minimum strain at 20 MPa confining stress).

The following points were noted from the study.

- The highest stress concentrations were not predicted to be at the core of the pillar at any of the depths modelled, but between the pillar core and the outer edges. This result suggests that most of the overburden load was not carried by the pillar core but by the entire pillar. For failure to occur,

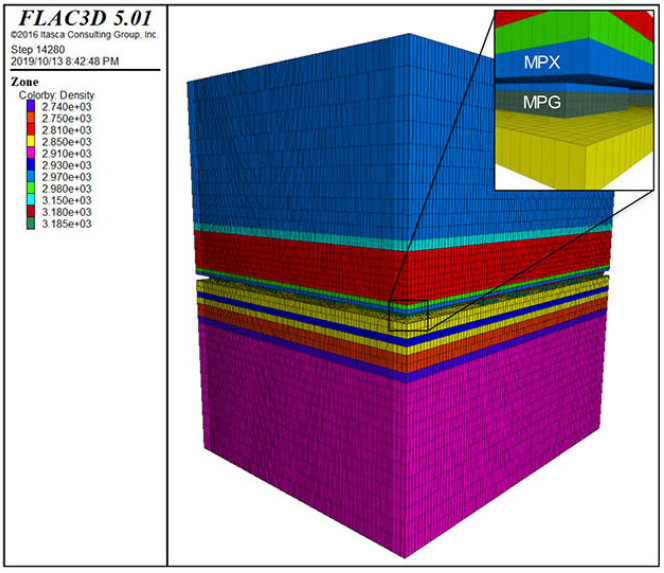

Figure 11—FLAC3D model showing the rock types immediately above and below the Merensky Reef

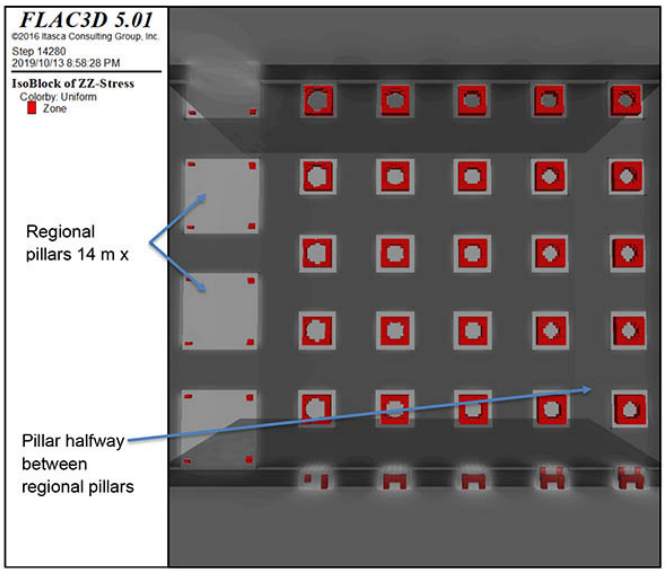

Figure 12—Plan view showing an iso-surface plot of the pillars where the vertical stress exceeds 195 MPa (red), 1270 m below surface

the pillar core must carry most of the load before the pillar reaches the peak stress of 195 MPa, under triaxial loading of at least 20 Mpa.

- As shown in Figure 12, no pillar load inversion was predicted for the specific scenarios modelled. However, should pillars start to slab and scale, further load shedding may occur, which would lead to stress being transferred to the core of the pillar. Fractured material around the pillars should preferably not be removed so as to ensure the long-term integrity of the pillar system.
- The 7 m × 7 m pillars with 7 m wide bords (and 11 bords between the 14 m × 14 m regional pillars) at 1270 m below surface were predicted to be stable.
- The layout using 7.5 m × 7.5 m pillars with 7 m wide bords (and 11 bords between the 14 m × 14 m regional pillars) was predicted to be stable down to 1310 m below the surface.

Table I

Minimum pillar widths for various depths below surface based on empirical and numerical modelling approaches

Depth (m)	Minimum pillar width (m) based on Hedley and Grant (1972), K-value 55 MPa	Modelled minimum pillar width for 7 m wide bords (m)
1270	14 × 14 (extraction ratio approx. 56%)	7 × 7 (extraction ratio approx. 65%)
1310	14 × 15 (extraction ratio approx. 55%)	7.5 × 7.5 (extraction ratio approx. 64%)
1350	14 × 15 (extraction ratio approx. 55%)	8 × 8 (extraction ratio approx. 64%)

- The layout using 8 m × 8 m pillars with 7 m wide bords (and 11 bords between the 14 m × 14 m regional pillars) was predicted to be stable down to 1350 m below the surface.

The modelling suggested that the minimum pillar widths could be significantly optimized based on the pillar load inversion and strain criterion concepts. A comparison of the empirical and modelling approaches is presented in Table I. Note the 9% difference in the extraction ratio between the two approaches (the loss associated with the regional pillars has been accounted for in the calculations). This pillar layout has been successfully implemented with zero pillar failures to date.

Case study 2: Pillar back-analysis: Simulation of pillar formation on the LG6 chromitite seam using monitoring data from an instrumented pillar

The pillars on another bord-and-pillar operation, in this case mining the Lower Group chromitite seam No. 6 (LG6), were initially designed in 1980 (van Zyl, 2023) using the Hedley and Grant empirical strength formula (1972). To gain a better understanding of LG6 pillar behaviour and develop representative rock mass parameters, an instrumentation programme was initiated in 2018 (van Zyl, 2023). Both the hangingwall and the footwall consist of pyroxenite, with a pyroxenite waste band separating the LG6 and LG6A chromitite seams.

A pillar back-analysis exercise was carried out using FLAC3D to simulate the stratigraphic sequence as described above, using the stress and deformation monitoring data obtained during the formation of an actual underground pillar, to calibrate the model. The mining steps and pillar formation were simulated, with model input parameters being adjusted until the measured strains and deformations aligned with the model results. For the back-analysis, the following parameters were varied: bulk modulus, shear modulus, cohesion, and friction angle. This calibration process ensured that the numerical models accurately reflected the actual behaviour of the rock mass.

An 8 m × 8 m pillar was monitored, located at a depth of 385 m below the surface, with 8 m wide bords and a mining height of approximately 3 m. The instrumentation included a CSIRO stress change monitoring cell placed at the centre of the pillar, as well as three displacement sensors positioned along the front (east) face of the pillar. These sensors recorded strain and displacement during various stages of pillar formation.

The strain and displacement data showed the structural integrity of the initial pillar and provided the opportunity for optimizing

Figure 13—Plan of the Kroondal mine MKF Section where the target (instumented) pillar was located (Smith and Piper, 2019)

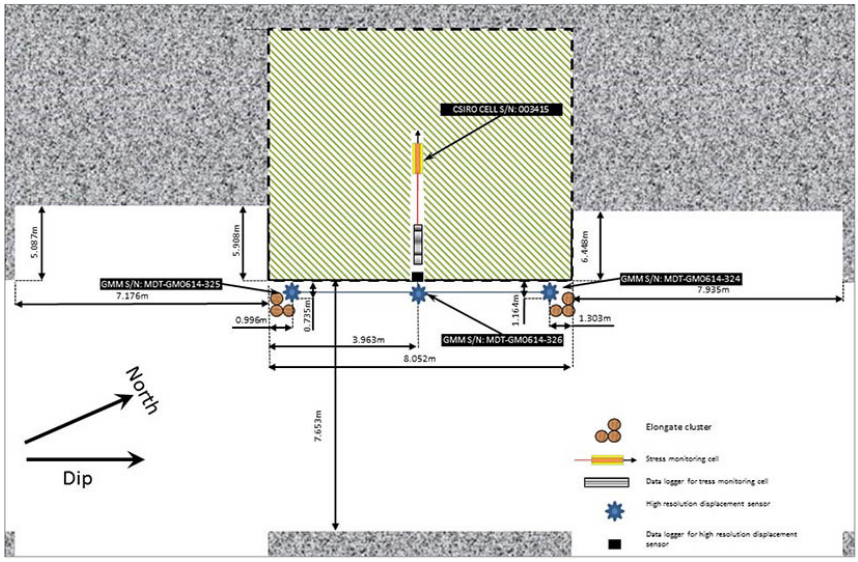

Figure 14—Layout of the instrumentation on the target pillar (Smith and Piper, 2019)

Figure 15—Sequence and dates of pillar formation (Le Bron and Piper, 2019)

the pillar system design for efficiency and safety. A mine plan of the section containing the target pillar was prepared before the pillar cutting, as shown in Figure 13. The target pillar, 91W22, was situated between the 90 West and 91 West bords.

The layout of the instrumentation is shown in Figure 14. The pre-mining vertical stress level was determined using the analytical formula based on the overburden density, gravitational acceleration, and depth below surface.

Figure 15 shows the extraction sequence and dates of extraction of the panels surrounding the target pillar. The first blast after the instruments were installed was on 19 September 2018 and the pillar was fully formed by 18 October 2018, nine blasts later. Numerous numerical iterations were run with a variety of rock mass properties used as input parameters. The Mohr-Coulomb constitutive model was used in FLAC3D until the combination of input parameters resulted in similar strain changes to those recorded underground.

The modelling results, shown in Figures 16–19, indicated the following.

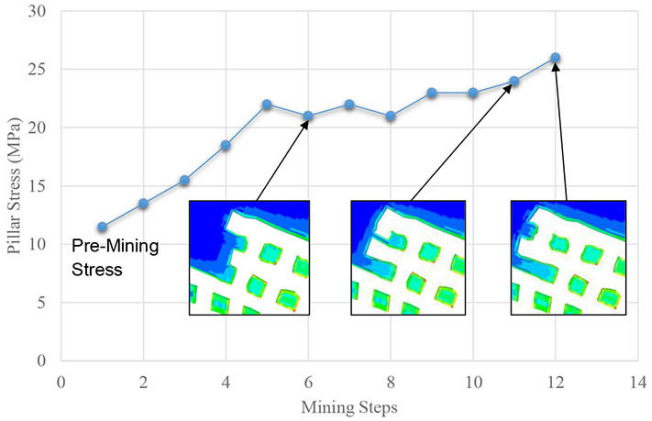

Figure 16—APS change during mining (mining steps 6, 11, and 12 layouts inserted)

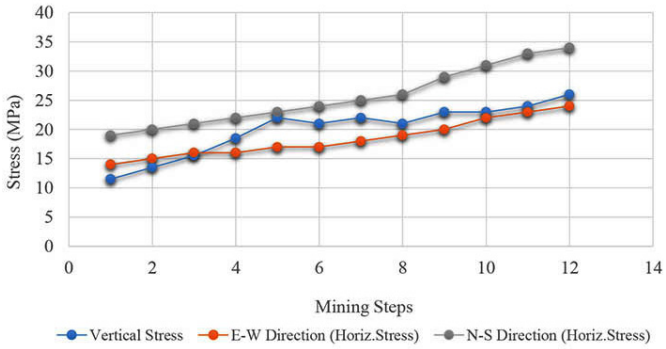

Figure 17—FLAC3D plot of stress in the target pillar

- The modelled vertical compressive stress in the instrumented target pillar increased from approximately 11 MPa (before mining) to 26 MPa (at the final mining step).
- The modelled stress changes are similar to those measured underground between 28 September 2018 (step 8) and 25 October 2018 (step 11) (Table II). Note that step 8 is when the four sides of the pillar had been established, although the pillar had not been completely formed (only three sides of the pillar had been established at step 7).

The modelling results can be summarized as follows.

- No pillar load inversion occurred in the target pillar.
- No loss of confinement occurred in the target pillar.
- No scaling of the target pillar was predicted.
- Based on the relatively small difference between the modelled and measured stress changes (between mining steps 8 and 12), the following can be inferred:
  - The back-analysed rock mass parameters, shown in Table III, are considered representative of the rock mass properties at the target pillar. These parameters were were used in the model that correlated best with the underground measurements, and recommended for future pillar stability analyses.
  - The *k*-ratios of approximately 1.8 in the N-S direction and 1.2 in the E-W direction appear to be representative of the stress regime at the target pillar.
- The target pillar was therefore assessed to be stable.

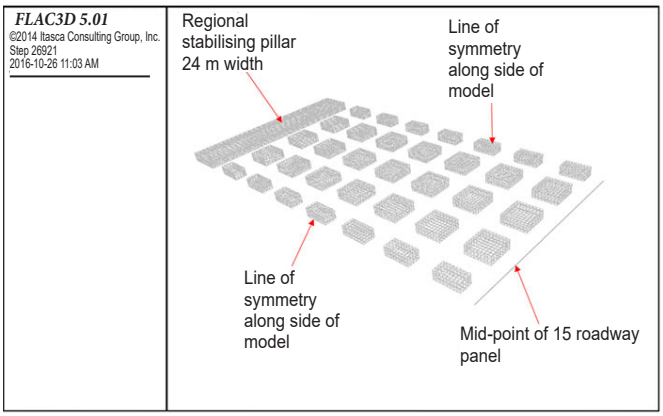

Figure 18—FLAC3D model outline of proposed pillars with a continuous regional stabilizing pillar. A vertical plane of symmetry was used on all four sides of the model

Case study 3: Application in a bord-and-pillar layout on the LG6 chromitite seam at depths of 370–500 m below surface

The assessment criteria for this case study were developed based on an extensive database of laboratory testing, stress measurement data, and mapping and core logging data.

- A strain criterion (for uniaxial loading conditions) of 1.1 mm/m was assigned to indicate the onset of fracturing, based on laboratory tests.
- A strain criterion (for triaxial loading conditions) of 3 mm/m was assigned to indicate the onset of fracturing under a confinement of 10 MPa (no triaxial loading data was available for the LG6 at the time of the study).
- A stress drop in the pillar core indicates pillar failure – loss of confinement may lead to disintegration.

Models of the proposed layout were run with regional stabilizing pillars of 24 m width, spaced 232 m apart skin-to-skin, with every fifth roadway cutting through the regional stabilizing pillar, and without regional stabilizing pillars. The in-stope pillars were 8 m × 8 m with 8 m wide bords, resulting in a 75% extraction ratio. A schematic showing the modelled layout is presented in Figure 18.

In-stope pillar behaviour at a depth of 370 m

The models showed that the vertical compressive strain is predicted to exceed the uniaxial compressive strain criterion of 1.1 mm/m on the sides of the pillars. However, at a confining load equalling or exceeding 10 MPa, the minimum strain in the core of the pillars was not predicted to exceed the criterion of 3 mm/m, as shown in

Table II

Comparison of measured and modelled stress changes in pillar (mining steps 8–12)

Measured (Mpa)			Modelled (Mpa)		
Vertical	Horizontal (E-W)	Horizontal (N-S)	Vertical	Horizontal (E-W)	Horizontal (N-S)
4.2	4.6	8.8	5	5	8

Table III

Back-analysed rock mass properties

Parameter	Hangingwall	LG6A	Waste	LG6	Footwall
Bulk modulus (GPa)	146	73	146	73	146
Shear modulus (GPa)	74	37	74	37	74
Cohesion (MPa)	6.0	3.2	6.0	3.2	6.0
Friction	50°	46°	50°	46°	50°
Tensile strength (MPa)	2.8	1.35	2.8	1.35	2.8

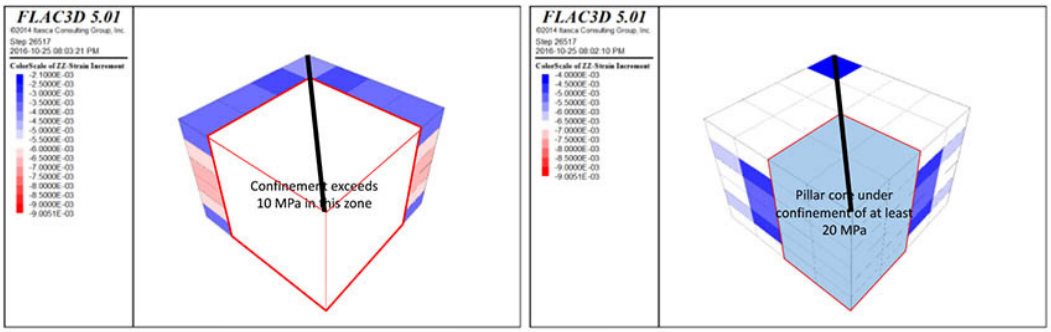

Figure 19 —Zones where confining stress levels of 10 MPa and 20 MPa are exceeded. The black line indicates the diagonal direction along which stresses were recorded in the model

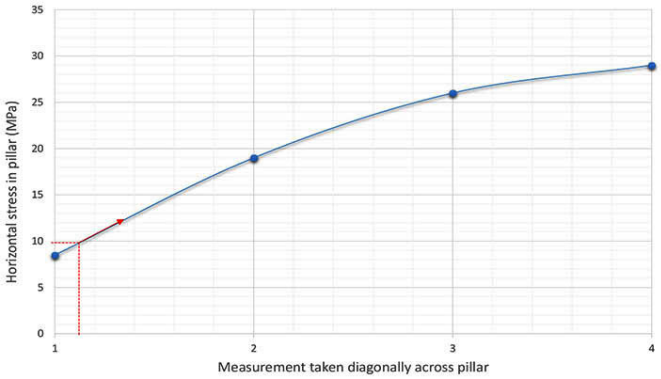

Figure 20 —Horizontal confining stress recorded in the FLAC3D model, diagonally across the pillar from the corner to the core. The criterion for indication of fracturing based on triaxial confinement of 10 MPa is 3 mm/m

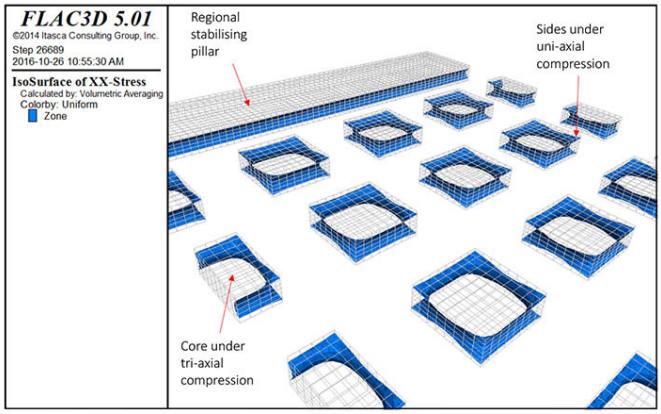

Figure 21—FLAC3D plot, where only the corners and sides of the LG6 pillars are exhibiting confinement of less than 5 MPa, at a depth of 370 m below surface with a regional stabilizing pillar

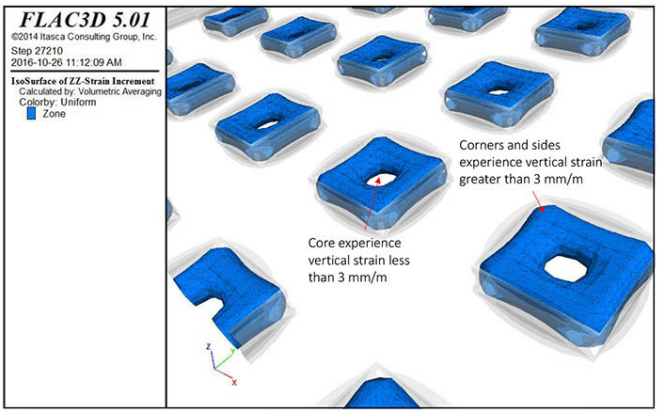

Figure 22—FLAC3D iso-surface with a vertical strain of 3 mm/m, at a depth of 370 m below surface with a regional stabilizing pillar. Note that the pillar core has not reached the 3 mm/m criterion

Figures 19–22. Thus 8 m × 8 m pillars with 8 m wide bords were predicted to remain stable at 370 m below the surface.

In-stope pillar behaviour for different mining heights at depths of 370 m and 500 m below surface

Based on available data, the thickness of the LG6 chromitite seam increases from 3 m at a depth of 370 m below surface to approximately 3.8 m at a depth of 500 m. The vertical virgin stresses were calculated at approximately 10.9 MPa at a depth of 370 m and 14.7 MPa at 500 m, representing an increase of 3.8 MPa or 34%.

A comparison of the modelling results of the pillar stresses at 370 m (3 m mining height) with those at 500 m (3.8 m mining height) shows that:

- Vertical stresses in the pillar cores increase from approximately 60 MPa (at a depth of 370 m below surface) to 140 MPa (at a depth of 500 m), which is more than 230%. The

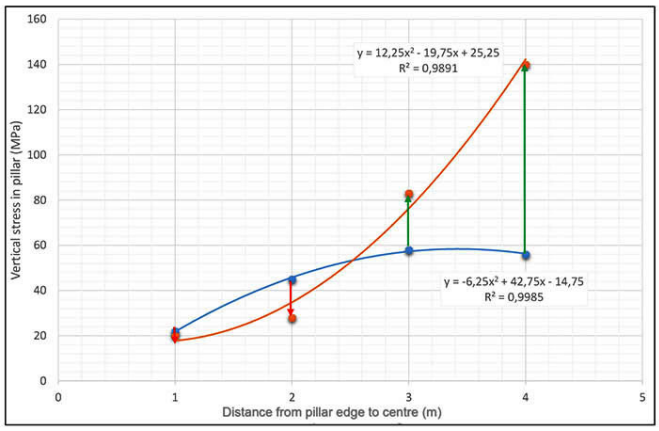

Figure 23—Vertical stress diagonally across two pillars at depths of 370 m (blue curve) and 500 m (orange curve) below surface

major reason appears to be the increase in pillar height, rather than the additional stress due to the depth increase.

- A slight stress drop is predicted to occur on the pillar sides, but not in the core, i.e. the sides of the pillars at 370 m experience slightly higher stress than the same sized pillars at a depth of 500 m. However, the vertical stress in the core of a pillar at 500 m below surface is significantly greater than that in the same pillar at a depth of 370 m.
- Partial pillar load inversion is predicted by the numerical model at a depth of 370 m below surface (Figure 23), which means that the pillar remains stable, albeit conditionally, i.e. possible future scaling of the sidewalls may push the pillar to full pillar load inversion. The pillars at 500 m depth are predicted to experience full pillar load inversion, meaning that the pillar has crushed – a precursor to potential failure.

Conclusions

The applicability of the hybrid methodology, which includes the empirical method, the consideration of pillar inversion, and the strain criteria based on uniaxial and triaxial loading conditions, to pillar stability assessments has been illustrated using three case studies.

The case studies include both shallow bord-and-pillar layouts and what would be considered 'deep' bord-and-pillar mining layouts. They clearly illustrate the impact of multiple parameters on pillar stability; including pillar height and rock mass strength (pillars on the Merensky Reef are similar in size to the pillars on the LG6, although the difference in mining depth is approximately 800 m), and the impact of regional pillars.

The use of this hybrid method of pillar stability assessment is recommended for pillar design, as the integration of different methods is often considered robust because it takes advantage of the strengths of each approach while mitigating their limitations. The more conservative empirical approach safeguards against possible unexpected factors (as a first step), while the numerical modelling approach enhances the understanding of pillar behaviour under simulated loading conditions. By proposing a process that starts with a conservative estimate of stability based on empirical methods, the method ensures a substantial safety margin.

Pillar back-analysis is required to enhance the reliability of pillar designs and forward predictions through the verification and adjustment of numerical models using real-world observations. This iterative process refines the comprehension of stress distribution, rock behaviour, and pillar performance. By optimizing the layout and dimensions of pillars based on these insights, mining operations can minimize risks, maximize safety, and enhance ore recovery.

References

Brady, B.H.G. and Brown, E.T. 1985. Rock Mechanics for Underground Mining. George Allen and Unwin, London. 527 pp.

Hedley, D.G.F. and Grant, F. 1972. Stope and pillar design for the Elliot Lake uranium mines. *CIM Bulletin*. vol. 65, pp. 37–44.

Hoek, E. and Brown, E.T. 1980. Empirical strength criterion for rock masses. *Journal of the Geotechnical Engineering Division, American Society of Civil Engineers*, vol. 106, pp. 1013–1035.

Itasca Consulting Croup. 2014. FLAC3D Version 5.01 Manual. Minneapolis, MN.

Kersten, R.W.O. 2019. An alternative pillar design methodology. *Journal of the Southern African Institute of Mining and Metallurgy*, vol. 119, no. 5, pp. 471–478.

Le Bron K.B. and Piper. P.S. 2019. Back analysis modelling of pillar formation at Kroondal Chrome Mine. Technical Consulting Report.

Lunder, P.J. and Pakalnis, R. 1997. Determining the strength of hard rock mine pillars. *CIM Bulletin*, vol. 90, pp. 51–55.

Malan, D.F. 2010. Pillar design in hard rock mines – Can we do this with confidence? *Proceedings of the Second Australasian Ground Control in Mining Conference*, Sydney, NSW. Australasian Institute of Mining and Metallurgy, Melbourne.

Napier, J.A.L and Malan, D.F. 2011. The design of stable pillars in the Bushveld Complex mines: A problem solved? *Journal of the Southern African Institute of Mining and Metallurgy*, vol. 111, no. 12, pp. 821–836.

Saiang, D., Gwynn, X., and Marshall, N. 2014. Hoek-Brown vs. Mohr-Coulomb – Results from a three-dimensional open-pit/underground interaction model. www.SRK.com.

Salamon, M.D.G. and Munro, A.H. 1967. A study of the strength of coal pillars. *Journal of the South African Institute of Mining and Metallurgy*, vol. 68, no. 2, pp. 55–67.

Smith, C. and Piper, P.S. 2019. The stress–strain behaviour of a stope pillar during formation at Kroondal Mine. Technical Consulting Report.

Spottiswoode, S.M. and Drummond, M. 2014. Pillar behaviour and seismicity in platinum mines. *Proceedings of the 6th Southern African Rock Engineering Symposium SARES 2014*, Misty Hills, Cradle of Humankind, South Africa. South African National Institute of Rock Engineering, Johannesburg.

Von Kimmelman, M.R., Hyde, B., and Madgwick, R.J. 1984. The use of computer applications at BCL Limited in planning pillar extraction and the design of mining layouts. *Design and Performance of Underground Excavations*. Brown, E.T. and Hudson, J.A. (eds). British Geotechnical Society, London. pp. 53–63.

Van Zyl, J. 2023. Personal communication. Glencore Kroondal Chrome Mine.

Watson, B. P., Lamos, R.A. and Roberts, D.P. 2021. PlatMine pillar strength formula for the UG2 Reef. *Journal of the Southern African Institute of Mining and Metallurgy*, vol. 121, no. 8, pp. 437–448 ◆